MASTER UCRL-15233

PSA 2619600

THE ROLE OF RADIATION DAMPING IN THE IMPEDANCE FUNCTION APPROACH TO SOIL-STRUCTURE INTERACTION ANALYSIS

NCT
ENGINEERING
INC.

May 1980

Prepared by: NCT Engineering, Inc.
For: University of California,
Lawrence Livermore Laboratory
Under: Personal Services Agreement 2619600

DISCLAIMER

This work was supported by the United States Nuclear Regulatory Commission under a Memorandum of Understanding with the United States Department of Energy.

THE ROLE OF RADIATION DAMPING IN THE IMPEDANCE FUNCTION APPROACH TO SOIL-STRUCTURE INTERACTION ANALYSIS

Prepared for University of California,
Lawrence Livermore Laboratory
P.O. BOX 308
Livermore, California 94550
Under Personal Services Agreement 2619600

Prepared by
NCT Engineering, Inc.
3650 Mt. Diablo Blvd. Suite 190
Lafayette, California 94549

May 1980

PREFACE

This report was prepared by N. C. Tsai of NCT Engineering, Inc., for the Lawrence Livermore Laboratory (LLL). It is intended to clarify certain technical issues in the analytical treatment of soil-structure interactions. These issues arose during the limited reanalyses of the Oyster Creek and Palisades Nuclear Power Plants that LLL is conducting for the U.S. Nuclear Regulatory Commission (NRC) as part of the Systematic Evaluation Program (SEP). The NRC FIN No. is A-0233, and the technical monitor is H. A. Levin.

The report is intended for use by the SEP's Senior Seismic Review Team in formulating recommendations on the treatment of damping in soil-structure interaction analysis. It has been technically reviewed by SEP program leaders R. C. Murray and T. A. Nelson at LLL.

The author wishes to thank Shelly Calvert for typing the final manuscript and R. K. Johnson of EG&G/San Ramon Operations for editing assistance.

ABSTRACT

This report was prepared at the request of the Lawrence Livermore Laboratory (LLL) to provide background information for analyzing soil-structure interaction by the frequency-independent impedance function approach. LLL is conducting such analyses as part of its seismic review of selected operating plants under the Systematic Evaluation Program for the U.S. Nuclear Regulatory Commission. The analytical background and basic assumptions of the impedance function theory are briefly reviewed, and the role of radiation damping in soil-structure interaction analysis is discussed. The validity of modeling soil-structure interaction by using frequency-independent impedance functions is evaluated based on data from several field tests. Finally, the recommended procedures for performing soil-structure interaction analyses are discussed with emphasis on the modal superposition method.

LIST OF SYMBOLS

C_x, C_r, C_v	Frequency-independent radiation damping coefficients for lateral translation, rocking and vertical translation of the base.
D_x, D_r, D_v	Radiation damping ratios based on C_x, C_r, and C_v, respectively.
K_x, K_r, K_v	Frequency-independent impedance springs for lateral translation, rocking and vertical translation of the base.
$C_{xx}(\omega)$, $C_{rr}(\omega)$	Frequency-dependent radiation damping coefficient for lateral translation and rocking of the base.
$K_{xx}(\omega)$, $K_{rr}(\omega)$	Frequency-dependent impedance springs for lateral translation and rocking of the base.
β_j, ω_j	Percentage of critical damping and natural frequency, respectively, of the j-th mode of the fixed base structure.
$\bar{\beta}_k$, $\bar{\omega}_k$	Composite modal damping and natural frequency, respectively, of the k-th mode of the soil-structure interaction system.
g	Gravitational acceleration.
G	Shear modulus of foundation soil.
V_s	Shear wave velocity of foundation soil.
ω	Circular frequency (radian/sec).

CONTENTS

1. INTRODUCTION

In the seismic analysis of structures, the soil-structure interaction effect may be accounted for by either the impedance function or the finite element approach. Both methods have advantages and limitations. Nevertheless, the state of the art indicates that both approaches share the same theoretical basis--specifically, both recognize that geometric radiation damping should be placed where the soil foundation is cut off from the soil-structure system. In the impedance approach, radiation damping is simulated by attaching to the structural base some frequency-dependent dampers or, if the approximation suffices, frequency-independent dampers. For the finite element approach, radiation damping is simulated by a series of dampers placed along the soil cut-off boundaries (e.g., Refs. 1, 2, 3, 4).

Unlike material internal damping, radiation damping is not an inherent material property. It is one of the parameters required to represent those soil media that are excluded from the soil-structure interaction model under consideration. Its analytical derivation is based on the assumption that the excluded soil media extended to a semi-infinite half space. In view of the relative dimensional difference between the earth and typical buildings, one may say that the half-space representation of the earth is fairly reasonable.

Note that the radiation damping concept has already been used in seismic prospecting and in investigating the influence of local soil deposits on earthquake ground motions (e.g., Refs. 5 and 6). Thus, it is a recognized way to account for the spatial dissipation of energy in a soil medium.

Over the last several years use of radiation damping in soil-structure interaction problems has gained acceptance by engineers. Much confusion still exists, however, for the following reasons:

- Many engineers do not have the background necessary to really understand the mechanism of radiation damping and to correctly apply the rather abstract concept to soil-structure interaction analyses. Radiation damping is often mistakenly perceived as a kind of material damping.
- It is generally held that the larger the radiation damping, the lower will be the structural response. As a consequence, limiting values on the magnitude of the radiation damping have been stipulated. Such confusion occurs because the actual effect of radiation damping on the structural response is seldom understood properly. As will be illustrated later in this report, an increase in radiation damping does not necessarily lead to a decrease in structural response.

- Data from dynamic tests of buildings and foundations provide the only realistic way to test the validity of soil-structure interaction theory. However, such data can often be misinterpreted. For example, one set of test data can lead to different conclusions depending on how the data are interpreted.
- Additional confusion arises in the simple case in which soil-structure interaction is represented by frequency-independent impedance functions. This is because most engineers use the method of modal superposition (also referred to as modal analysis or the normal mode method) to solve the equations of motion, but few realize that:
  - Modal superposition gives only approximate solutions; the rigorous solution must be obtained by such methods as Fourier transformation or direct integration.
  - The computed structural response may vary appreciably with the technique chosen for determining the composite modal damping.
  - Modal superposition is inapplicable, no matter what modal damping values are used, for cases in which the radiation damping is sufficiently large. This will be illustrated later in the report.

  Such misunderstandings lead many engineers to stipulate a limiting value for the composite modal damping, giving rise to yet another controversy.

This report is intended to review the impedance function approach and the significance of radiation damping in soil-structure interaction analyses and, thereby, to clarify the issues described above. To accomplish these objectives, the report is organized as follows:

- Brief review of the essence of the impedance function representation for a foundation.
- Discussion of the effect of radiation damping on structural response.
- Discussion of the limitations of the modal superposition method and the proper view of the role of composite modal damping in the analysis.
- Evaluation of the available dynamic field test data and their correlation with theory.

2. THE IMPEDANCE FUNCTION APPROACH

For a structure founded at the surface of a site that is idealized as an elastic, horizontally layered half space (Fig. 2-1(a)), the half-space foundation may be analytically represented by a set of complex, frequency-dependent impedance functions. In essence, the impedance functions relate the structural base shear and moment--$V_b(t)$ and $M_b(t)$, respectively--to the base motions as follows

$$\begin{Bmatrix} V_b(t) \\ M_b(t) \end{Bmatrix} = \begin{bmatrix} R_{xx}(\omega) + iI_{xx}(\omega) & R_{xr}(\omega) + iI_{xr}(\omega) \\ R_{rx}(\omega) + iI_{rx}(\omega) & R_{rr}(\omega) + iI_{rr}(\omega) \end{bmatrix} \begin{Bmatrix} x_b(t) \\ r_b(t) \end{Bmatrix} \qquad (2\text{-}1)$$

where x_b is the base translation relative to the free-field motion, and r_b is the base rotation.

The impedance functions are frequency-dependent because the soil mass is included in the derivation. The imaginary parts in the impedance matrix exist because of the assumption that certain refracted seismic waves propagate into the semi-infinite space and do not return; they vanish identically if, instead, a perfectly rigid boundary is assumed to exist somewhere in the half-space soil foundation. The off-diagonal terms are usually small and, as a simplification, may be ignored. As a mechanical analogy, the simplified impedance matrix may be translated into a set of frequency-dependent springs and dampers by letting

$$\begin{aligned} R_{xx}(\omega) &= K_{xx}(\omega) & I_{xx}(\omega) &= \omega C_{xx}(\omega) \\ R_{rr}(\omega) &= K_{rr}(\omega) & I_{rr}(\omega) &= \omega C_{rr}(\omega) \end{aligned} \qquad (2\text{-}2)$$

Thus, the simplified Eq. (2-1) can be rewritten (Ref. 7) as

$$\begin{Bmatrix} V_b(t) \\ M_b(t) \end{Bmatrix} \cong \begin{bmatrix} K_{xx}(\omega) & \\ & K_{rr}(\omega) \end{bmatrix} \begin{Bmatrix} x_b(t) \\ r_b(t) \end{Bmatrix} + \begin{bmatrix} C_{xx}(\omega) & \\ & C_{rr}(\omega) \end{bmatrix} \begin{Bmatrix} \dot{x}_b(t) \\ \dot{r}_b(t) \end{Bmatrix} \qquad (2\text{-}3)$$

This results in the equivalent soil-structure system shown in Fig. 2-1(b), in which the impedance functions K_{vv} and C_{vv} are for vertical vibrations.

When the soil profiles permit a uniform half-space idealization of the site, the frequency-dependent parameters may be further approximated by

frequency-independent ones (Ref. 7). That is, Eq. (2-3) may be further simplified for a uniform site:

$$\begin{Bmatrix} V_b(t) \\ M_b(t) \end{Bmatrix} \equiv \begin{bmatrix} K_x & \\ & K_r \end{bmatrix} \begin{Bmatrix} x_b(t) \\ r_b(t) \end{Bmatrix} + \begin{bmatrix} C_x & \\ & C_r \end{bmatrix} \begin{Bmatrix} \dot{x}_b(t) \\ \dot{r}_b(t) \end{Bmatrix} \tag{2-4}$$

Because of the approximation, the values of $K_x,\ldots,C_r$ may vary somewhat, depending on the choice of the individual engineer. A popular choice is that suggested by Richart, Hall, and Woods (Ref. 8). Tables 2-1 an 2-2 show their values for circular and rectangular bases, respectively.

Several important features of the impedance functions are summarized below.

(a) The impedance functions are analytically derived on the assumptions that the structural base is rigid and that a perfect bond exists between the base and the soil foundation. For actual building bases that have a large ratio of horizontal dimension to thickness, the rigid-base assumption may be questionable. However, the "box" or "framing" effect of those structural walls extending down to the base tends to increase base rigidity. In other words, the base slab within a building system is actually more flexurally rigid than if the base slab alone is placed on the soil foundation. Such an observation has typically been demonstrated by finite element soil-structure interaction analyses for which no rigid-base assumption is necessary.

(b) As pointed out above, the equivalent damping terms in the impedance functions stem from the imaginary parts that exist because of the wave radiation assumption in the theory. Therefore, they should not be construed as material damping.

(c) The impedance functions represent the equivalent boundary conditions required to replace the entire half-space foundation that is excluded from the model along the soil-structure interface. In the event that the half-space foundation is cut off somewhere away from the base--such as in the finite element approach--the impedance functions required along the cut-off boundary to replace the excluded portion of the foundation become those described in Ref. 1. The soil-structure system shown in

Fig. 2-1(c), therefore, is mathematically identical to those in Figs. 2-1(a) and (b). This illustrates the statement made in the Introduction that both the impedance and the finite element approaches share the same theoretical basis--the half-space assumption.

(d) The effect of soil material damping may be accounted for in the impedance functions through analytical derivations (Refs. 9, 10). The soil damping mechanism may be viscous or hysteretic.

Inclusion of the material damping modifies both the spring and the damping terms, although, as one would anticipate, the effect on the latter is more pronounced. The equivalent damping terms now contain the composite effects from both the radiation damping and the material damping.

(e) Rigorous analytical solutions are not available yet to account for the effect of structural embedment. Approximate solutions, however, have been suggested (e.g., Refs. 10, 11). In general, embedment tends to increase the values of both the spring and the damping terms.

TABLE 2-1. Frequency-independent impedance functions for circular bases (from Ref. 8).

Motion	Equivalent Spring Constant	Equivalent Damping Coefficient
Horizontal	$K_x = \frac{32(1-\nu)GR}{7-8\nu}$	$C_x = 0.576 K_x R \sqrt{\rho/G}$
Rocking	$K_r = \frac{8GR^3}{3(1-\nu)}$	$C_r = \frac{0.30}{1+B_\psi} K_x R \sqrt{\rho/G}$
Vertical	$K_v = \frac{4GR}{1-\nu}$	$C_v = 0.85 K_v R \sqrt{\rho/G}$

ν = Poisson's ratio of foundation medium,

G = shear modulus of foundation medium,

R = radius of the circular base mat,

ρ = density of foundation medium,

$$B_\psi = \frac{3(1-\nu)I_o}{8\rho R^5},$$

I_o = total mass moment of inertia of structure and base mat about the rocking axis at the base.

TABLE 2-2. Frequency-independent impedance functions for rectangular bases (*from Ref. 8*).

Motion	Equivalent Spring Constant	Equivalent Damping Coefficient *
Horizontal	$K_x = 2(1+\nu)G\beta_x\sqrt{BL}$	$R_x = \sqrt{BL/\pi}$
Rocking	$K_r = \frac{G}{1-\nu}\beta_\psi B^2 L$	$R_r = \sqrt[4]{B^3 L/3\pi}$
Vertical	$K_v = \frac{G}{1-\nu}\beta_z\sqrt{BL}$	$R_v = \sqrt{BL/\pi}$

* The equivalent radius, R_x, R_r or R_v is for computing the radiation damping C_x, C_r or C_v, respectively, using the Table 2-1.

B = width of the base mat in the plane of horizontal excitation;

L = length of the base mat perpendicular to the plane of horizontal excitation;

β_x, β_ψ, β_z = constants that are functions of the dimensional ratio, B/L. (After Fig. 10-16 in Ref.8)

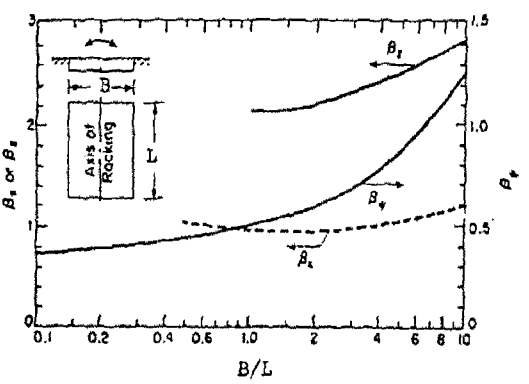

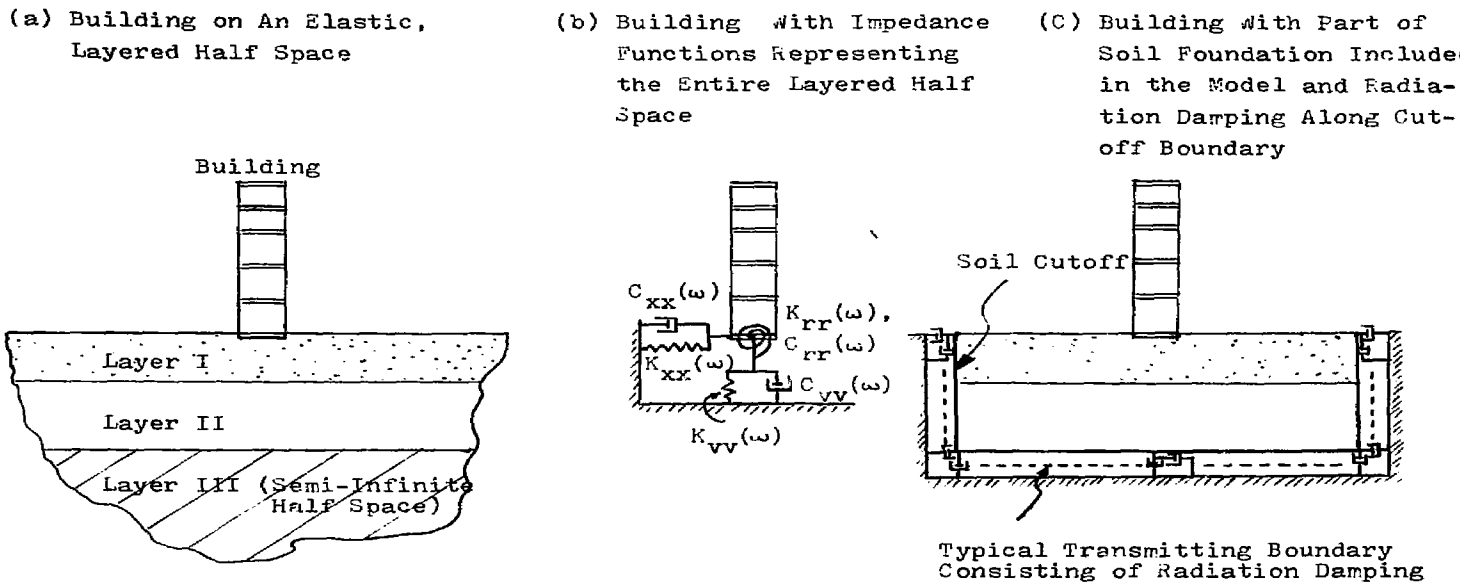

Fig. 2-1 The Three Mathematically Equivalent Soil-Structure Systems

3. RADIATION DAMPING

This section details the pitfalls of expressing radiation damping in terms of a damping ratio that is then used to predict the effect of radiation damping on structural response. A simple illustrative example of a one-mass structure is presented.

3.1 RADIATION DAMPING AS A DAMPING RATIO

It is common engineering practice to convert the radiation damping coefficient that is derived from theory into a certain damping ratio in order to predict its effect on the structural response. This practice may have begun because engineers are familiar with the concept of the modal damping ratio as a convenient measure of the effect of material damping in a structural system subjected to dynamic loadings. There are several pitfalls associated with treating radiation damping the same way, and few engineers actually know about them. These pitfalls are discussed below.

(a) To convert the radiation damping coefficient, say C_x, into a damping ratio requires a certain definition such as

$$D_x = C_x/2\sqrt{km} \qquad (3\text{-}1)$$

This definition applies only to single-degree-of-freedom (SDOF) systems having uniquely specified values of m, c, and k, and it has certain physical meaning. A question hence arises: what k and m must be used in Eq. (3-1) for a soil-structure system? There is no unique answer to this question; hence, the value of D_x will vary depending on the engineer's choice. Although one common practice is to use $k = K_x$ and m = total structural mass, the D_x so computed has no particular physical significance unless the struture is so stiff relative to K_x that it may be regarded as a rigid body, and the entire interaction system may be viewed as a SDOF system.

In short, not only does D_x have no unique definition, it generally has no particular physical meaning. Thus, misunderstanding and misuse of the radiation damping concept can easily happen whenever it is thought of only in terms of the damping ratio.

(b) Not realizing that the theory provides only the radiation damping coefficient from which the damping ratio must be computed, many engineers infer that structures with similar geometry and founded on similar soils have similar values of radiation damping ratios for soil-structure interaction analyses. The pitfall is apparent: it is the radiation damping coefficients that would have similar values. Consider the conditions shown in Fig. 3-1. For Case (a), which consists of the basemat alone, assume that D_x equals 18% as predicted by the theory or measured from dynamic tests. According to the theory, the value of the radiation damping coefficient, C_x, will remain the same for all three cases. Applying Eq. (3-1) to convert to a damping ratio and using the conventional practice of $k = K_x$ and m = the total structural mass, one would find that the same C_x results in the following D_x values:

$$D_x = 18\%/\sqrt{4} = 9\% \quad \text{..... Case (b)}$$
$$D_x = 18\%/\sqrt{9} = 6\% \quad \text{..... Case (c).}$$

Note that K_x remains unchanged for all three cases, according to the theory; hence, D_x is inversely proportional to the total structural mass in this example. To infer that all three cases have the same value of $D_x = 18\%$ is apparently erroneous.

(c) Many engineers take D_x to be a modal damping ratio to predict how radiation damping affects structural response. This misunderstanding will be clarified in Sec. 3.2.

(d) As mentioned in the Introduction, engineers often resort to modal superposition for the numerical solution in analyzing uniform soil sites, for which the impedance functions are approximate frequency-independent functions. Certain composite modal damping values must then be determined, and computational techniques have been developed that are formulated only in terms of the radiation damping ratio, not the damping coefficient. The pitfall associated with adopting such techniques to calculate composite modal damping will be discussed in Sec. 4.

3.2 THE EFFECT OF RADIATION DAMPING

It is generally held that large radiation damping results in low structural response. Such is not necessarily true, and the illusion stems from a misunderstanding of the actual role of radiation damping. To illustrate this point, consider one simple example--a two-mass, spring-and-damper-connected system undergoing vertical harmonic vibrations as depicted in Fig. 3-2. The system may be regarded as a soil-structure interaction system composed of a one-mass structure (m_1), the base (m_2), and the frequency-independent impedance functions k_2 and c_2. The structural frequency is 5 Hz, and structural damping is 2% of critical (see Fig. 3-2). Let c_2, the radiation damping in this case, be a variable which, when converted to the dimensionless parameter D_2 according to Fig. 3-2, assumes the values of 0.1, 0.5, 1, 2, 5 and 10. When subjected to harmonic, vertical, input ground motion of $\ddot{u}_g(t) = \sin \omega t$, the amplitude of the steady-state response of m_1 is that shown in Fig. 3-3 (Ref. 12). Note the following observations.

- The response amplitude of m_1 indeed decreases as D_2 increases from 0.1 to 0.5 to 1.0, but then it increases again for higher values of D_2.
- The resonant frequency of the system, which is dictated by the location of the peak frequency for the amplitude curve of m_1, shifts from 3.8 Hz (the first frequency of the undamped system) to 5 Hz (the fixed-base-structure frequency) as D_2 increases from 0.1 to 10.0. This is so because the dynamic response of m_1 approaches that of the fixed-base structure as D_2 becomes large. In the limiting case (D_2 becomes infinite), the structure becomes dynamically fixed at the base because of the infinite damping force, even though spring k_2 has only a finite value. In other words, the amplitude curve of m_1 for D_2 equals infinity will be identical to that of the fixed-base structure having a damping of 2% critical.

The point to be made here is that the radiation damping ratio is merely a dimensionless quantity and, unlike the modal damping, cannot be used to predict the magnitude of the structural response. The example clearly demonstrates another important point: arbitrarily reducing the magnitude of the radiation damping for any given problem for fear that the structural response might be underestimated does not necessarily produce a more

conservative structural response. Besides, such a reduction may result in a floor spectrum that has peaks at erroneous frequencies. For instance, assume that the theoretical value of D_2 is actually 10 in the example problem. If this value is drastically reduced to 0.1, the response of m_1 would not increase drastically as many would anticipate. Actually, the response of m_1 decreases slightly. Also, the resonant frequency is in error (3.8 rather than 5.0 Hz).

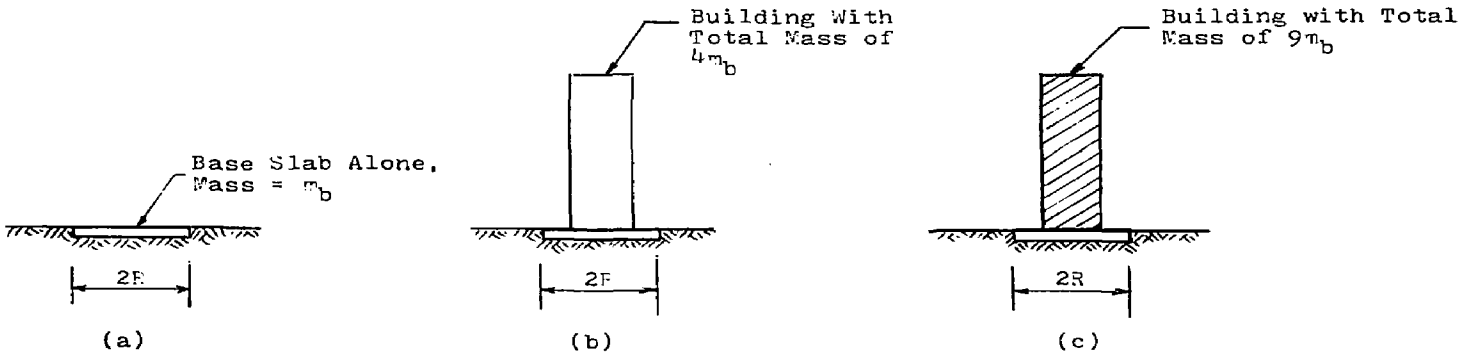

Fig. 3-1 Three Structures Founded on Identical Soil Foundation Media , Having Identical Base Dimension But Different Mass

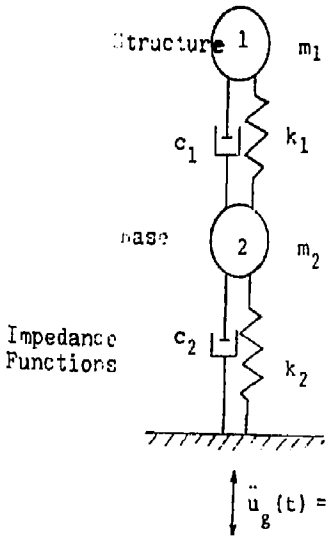

$m_1 = m_2 = 1$ kip-sec^2/ft

$\sqrt{k_1/m_1} = 10\pi$ rad/sec (= 5 Hz)
= fixed base structural frequency

$c_1/2\sqrt{k_1 m_1} = 2\%$

$\sqrt{k_2/(m_1+m_2)} = 10\pi$ rad/sec (= 5 Hz)

$D_2 = c_2/2\sqrt{k_2(m_1+m_2)}$ = Variable Parameter

Frequencies of the 2-mass system :

$\bar{\omega}_1 = 3.8$ Hz

$\bar{\omega}_2 = 9.2$ Hz

Fig. 3-2 The One-Mass Structure and Soil Interaction System for Vertical Vibrations

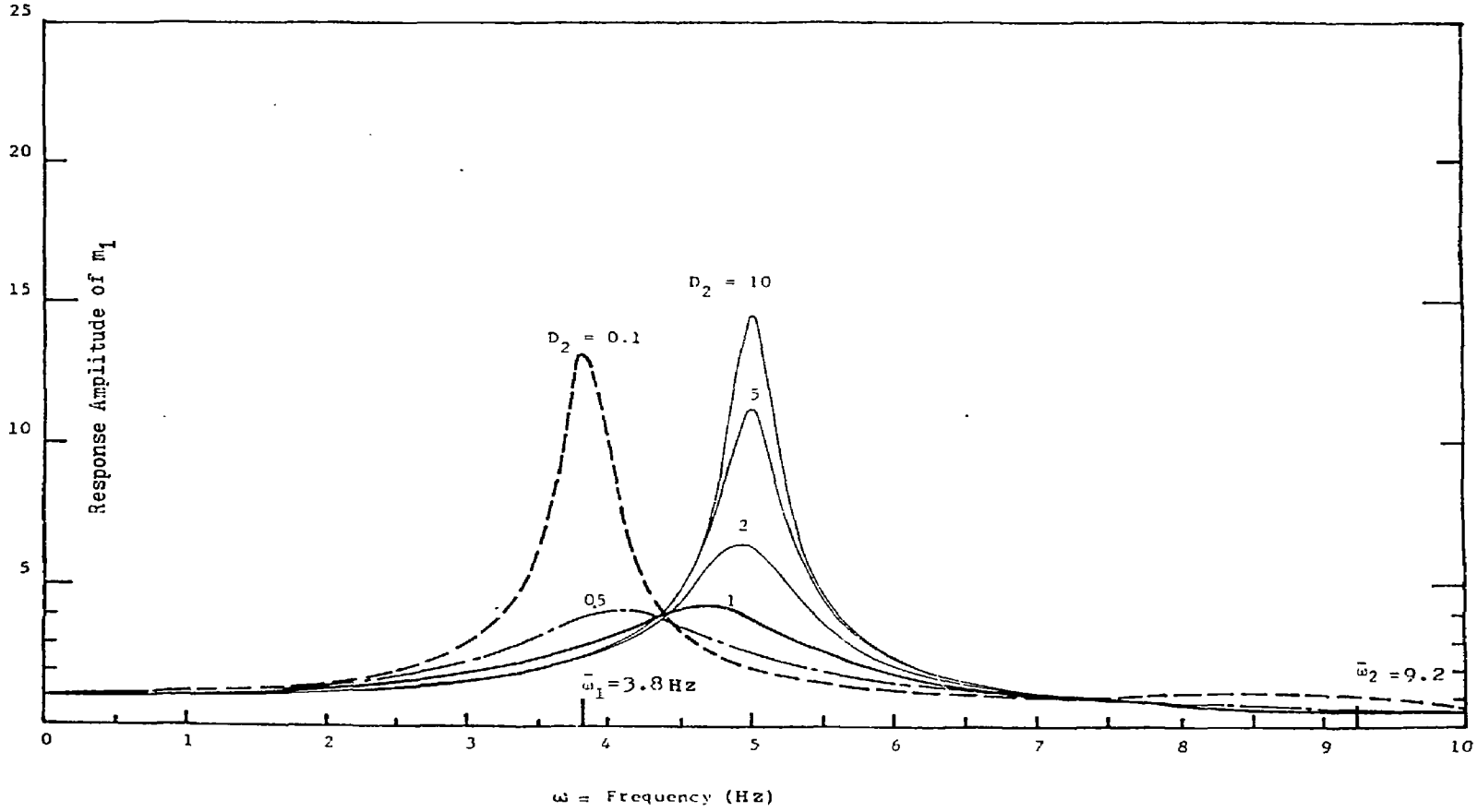

Fig. 3-3 Response Amplitude of m_1 As a Function of Excitation Frequency ω and D_2

4. RESPONSE ANALYSIS BY THE METHOD OF MODAL SUPERPOSITION

In the impedance approach to soil-structure interaction analysis, the equations of motion should explicitly incorporate the impedance springs, K, and dampers, C, in the system stiffness and damping matrices, respectively. Moreover, when the damping property of the structure is specified in terms of the fixed-base structural modal damping, which is the current practice, a certain transformation of the coordinates must be applied to the equations of motion so that the structural modal frequences, ω_j, and damping values, β_j, are explicit parameters in the transformed system stiffness and damping matrices, respectively (e.g., Ref. 13).

In general, because the impedance springs and dampers are frequency-dependent, the equations of motion are solved rigorously by the method of Fourier transformation in the frequency domain. When frequency-independent impedances can be used for uniform soil sites, for example, the rigorous solution can be obtained by the methods of Fourier transformation, complex modal analysis, or direct integration. The method of normal mode superposition, though widely used in engineering practice, yields only approximate solutions because classical normal modes do not exist, in general, for the problem under consideration. Besides, under certain conditions the normal mode approximation may be unacceptable--a very important point.

In conjunction with the application of modal superposition, controversies arise with regard to the technique for determining the composite modal damping, $\tilde{\beta}_k$, and its magnitude. It has often been postulated that the composite modal damping value should be limited in order to produce conservative structural response.

This section highlights the limitations of modal superposition for soil-structure interaction analysis. A proper understanding of the role of the composite modal damping in such analyses is developed.

4.1 LIMITATIONS

The very nature of modal superposition dictates that the resonant frequencies of the structural response invariably coincide with the frequencies of the soil-structure system, $\tilde{\omega}_k$. As illustrated previously in Fig. 3-3, the resonant frequencies of the system will gradually increase

toward the fixed-base structural frequencies, ω_j, as the radiation damping increases. Such a frequency shift cannot be done with normal mode methods, no matter what composite damping values are used. To illustrate this point, consider again the two-mass system in Fig. 3-2.

Figure 4-1 shows the normal mode solutions for the response amplitude of structural mass m_1 for several assumed composite modal damping ratios, $\bar{\beta}_1$ and $\bar{\beta}_2$. A close comparison of Fig. 4-1 and Fig. 3-3 reveals the following:

(a) When $D_2 = 0.1$ (damping ratio for the foundation), the normal mode approximation is acceptable, and the required values for composite modal damping are, by inspection, $\bar{\beta}_1 \cong 4\%$ and $\bar{\beta}_2 \cong 40\%$.

(b) When D_2 exceeds 0.5, the normal mode approximation becomes less acceptable, regardless of the values of the composite modal damping. In fact, when D_2 exceeds 1.0, a fixed-base-structure assumption turns out to be a better approximation, provided that an effective structural modal damping greater than 2% is used. As D_2 increases further, the effective damping rapidly converges toward 2%--the fixed-base structural damping specified initially.

In conclusion, modal analysis should be used with caution because its validity largely depends on the magnitude of the radiation damping and the structural rigidity relative to impedance springs. Provided that the relative structural rigidity is not too great, the modal superposition approximation is generally acceptable until the radiation damping, expressed in terms of the dimensionless ratio D, exceeds the range of 0.8 to 1.0.

4.2 COMPOSITE MODAL DAMPING

4.2.1 Determination of Composite Modal Damping

When the impedance functions permit the normal mode approximation, the value of the composite modal damping also dictates how close are the amplitudes of the approximate and rigorous solutions. Several techniques are available for estimating modal damping values (e.g., Refs. 13, 14, 15). These methods are not compared at great length here. Note, however, that a suitable technique must always correlate the approximate and rigorous solutions during

the process of computing the composite modal damping (e.g., Ref. 13). Although the correlation criteria may vary from one person to another, the variation is usually small, and one can always foretell the quality of the approximation with respect to the rigorous solution. For instance, the best estimates for $\bar{\beta}_1$ and $\bar{\beta}_2$ for the two-mass system discussed in Sec. 4.1 (a) were based on correlating the approximate and rigorous solutions for the response of m_1.

On the other hand, any technique that computes the composite modal damping without a correlation with the rigorous solution will render the degree of approximation uncertain. This is the case with most existing techniques (e.g., Refs. 14, 15). Typically, these techniques compute the composite modal damping as a certain weighted average of the structural damping β_j and the radiation damping ratios, D_x, and D_r. A convenience, and, hence, a defect, of these techniques is that they do not require formal formulation of the equations of motion. The nonuniqueness of the parameters, D_x and D_r, adds additional uncertainty to the computed damping values. A general trend has been observed--these techniques usually overestimate the required modal damping and, hence, underestimate the structural response, particularly when the radiation damping ratios are much larger than the structural damping (Refs. 13, 14).

4.2.2 The Proper Role of Composite Modal Damping

To understand the role of the composite modal damping, it is imperative to first observe the following premise:

> Given that the impedance functions are valid representations of the foundation, that the rigorous solution must be obtained by one of the three numerical analysis methods mentioned above, and that normal mode approximation is permissible, then the required composite modal damping values, regardless of their magnitudes, must be set in such a way that the optimum approximation for the structural response can be achieved.

Thus, to arbitrarily limit the computed values of the composite damping is, in reality, to render a poor approximate solution. Unnecessary conservatism will be introduced into the structural response, and sometimes extra floor spectrum peaks will be created with respect to the rigorous solution. For example, consider again the two-mass system. For the case of $D_2 = 0.1$, the best estimates for $\bar{\beta}_k$ are, according to Sec. 4.1 (a), $\bar{\beta}_1 \cong 4\%$ and $\bar{\beta}_2 \geq 40\%$.

Say $\bar{\beta}_2$ is to be reduced to 10%. Then, the consequence is obvious: based on Fig. 4-1, an extra spectral peak having an appreciable amplitude could be created at $\bar{\omega}_2$ = 9.2 Hz on the floor spectrum of m_1.

In general, unless the radiation damping is small, at least two modes (one mode for vertical analyses) are inevitably associated with large values of composite modal damping. These are the modes for which substantial participation of the base translation and/or base rocking takes place, which is physically understandable. For a given problem, if such modes do not occur within the frequency range of interest, it does not mean that they do not exist. They are at higher frequencies.

4.3 CASE STUDY

Reference 16 presents a very interesting case study of the structure-foundation interaction effect for a seven-story braced truss chime tower (Fig. 4-2). A frequency sweeping test was done with a shaker placed on the fourth floor. Apparent resonances were observed at about 2.4 to 2.5 Hz and at 7.9 to 8.5 Hz, and the associated damping values were estimated to be about 2.5% and 5.5%, respectively.

The authors then established a mathematical model for the structure and attempted an analytical correlation with the field test results. Two different approaches were used. In the first approach, the soil-structure interaction effect was simply assumed to be negligible, and a fixed-base model was considered. The frequencies of the first two modes of the fixed-base model are compared with the measured values in Fig. 4-3. The correlation is reasonably good, indicating that the interaction effect is indeed insignificant. As one may anticipate, the analytical modal frequencies are slightly higher than the test results because the deformability of the foundation soil was neglected.

In the second approach, frequency-independent impedance springs, K_x and K_r, were computed to represent the foundation. The frequencies and mode shapes of the first three modes are shown in Fig. 4-3. Note that the second mode (4.7 to 6.9 Hz) was not observed in the field tests, nor in the fixed-base model. This by no means implies that the interaction model is inaccurate, because the first and third modes agree closely with the test results. The only logical interpretation is that the second mode must be highly damped. Such an interpretation is supported by the fact that the

second mode shape is predominantly translation and rocking of the base, and, hence, a high damping for that mode is anticipated. Though the authors did not attempt to compute the composite modal damping, they estimated that the second mode must have a damping of at least 50%.

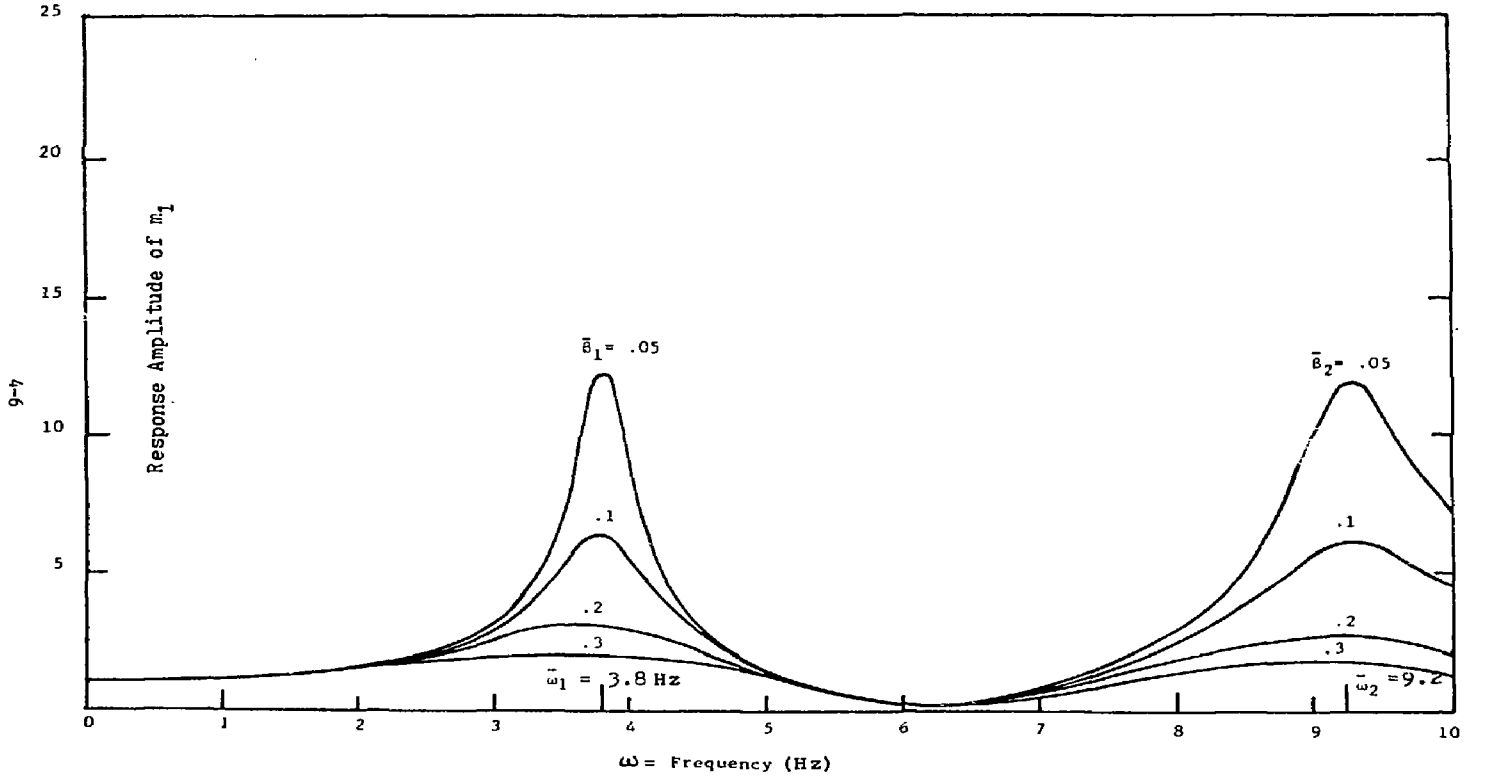

Fig. 4-1 Normal Mode Approximation for Amplitude of m_1 As a Function of $\bar{\beta}_1$ and $\bar{\beta}_2$

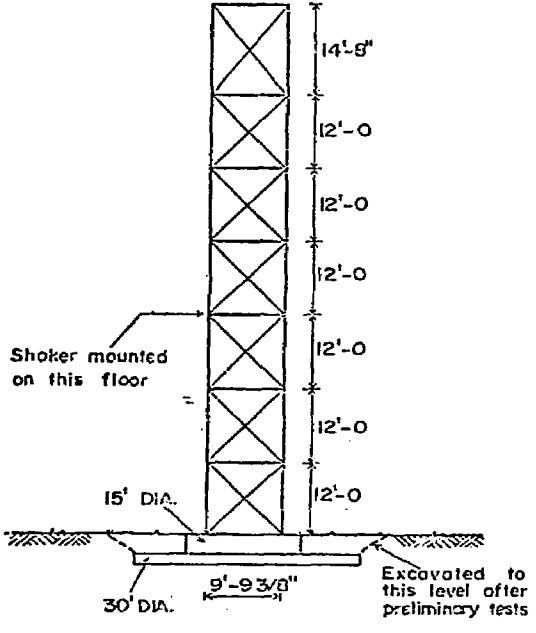

Fig. 4-2
ELEVATION OF CHIMES TOWER
(reproduced from Ref. 16)

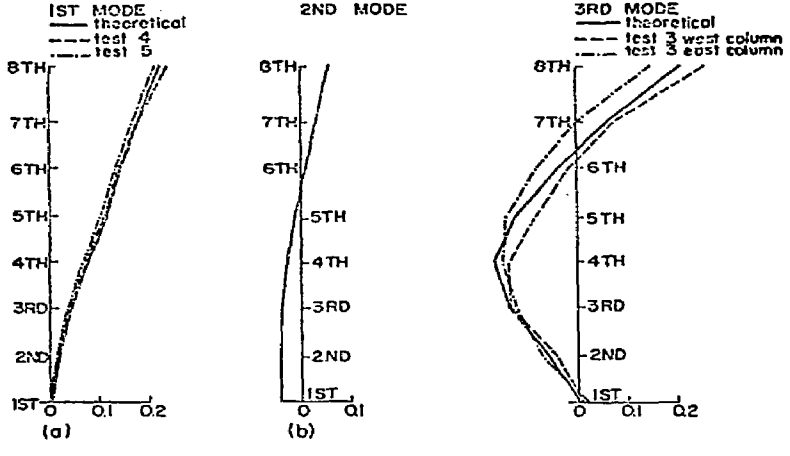

Fig. 4-3 COMPUTED AND OBSERVED MODE SHAPES
(reproduced from Ref. 16)

	Calculated		
	Fixed base		With interaction
Observed	Nielsen(2.3)	Writers	Writers
2.4-2.5	2.8	2.76	2.41-2.44
			4.73-6.01
7.9-8.5	9.2	8.95	8.76-8.97

5. EVALUATION OF FIELD TESTS

In this section, information from several available dynamic field tests is reviewed to assess the validity of the impedance theory. Of particular interest is the evaluation of the analytical radiation damping values in Tables 2-1 and 2-2, which, though often used, are extremely controversial.

Some field tests were performed on structures, others on footings. It is important to differentiate the two. The damping ratio deduced from tests on structures is equivalent to the composite modal damping for the interaction system, $\tilde{\beta}_k$, while that from tests on footings is equivalent to the defined damping ratio, D, which comprises the combined effects of radiation damping and soil material damping. Each available test result is reviewed separately below.

5.1 CASE I--HAMAOKA NO. 1 BWR REACTOR BUILDING (Ref. 17)

5.1.1 Structural Data

Base dimension	:	64 m x 64 m
Total wt. (mg)	:	1.44×10^5 ton
Mass mom. inert. abt. base (I_o)	:	9.916×10^6 t-m-sec^2
Total height	:	58.7 m
Embedment	:	12.7 m on three sides

5.1.2 Foundation Data

Shear wave velocity (V_s)	:	800 m/sec on ave.
Shear modulus (G)	:	1.312×10^5 t/m^2
Unit weight (ρg)	:	2.01 t/m^3
Poisson's ratio	:	1/3

5.1.3 Analytical Impedances

From Table 2-2, the equivalent radii for calculating the radiation damping are R_x = 36.2 m and R_r = 36.6 m, and the following were computed:

$$K_x = 2.24 \times 10^7 \text{ t/m}$$
$$D_x = \underline{51\%} \quad (D_x = C_x / 2\sqrt{K_x m})$$
$$K_r = 2.58 \times 10^{10} \text{ t-m/rad}$$
$$D_r = \underline{31\%} \quad (D_r = C_r / 2\sqrt{K_r I_o})$$

The authors did a complete analytica. ediction of the composite modal damping, using the frequency-dependent im nce functions suggested by Tajimi (Ref. 18) for a uniform half space. Figure 5-1 compares the simplified, frequency-independent impedances with the frequency-dependent impedances. Note that for horizontal motions $K_1(\omega)$ is to be compared with K_x, and $K_2(\omega)$ with ωC_x. Similarly, for rotational motions $K_1(\omega)$ is to be compared with K_r, and $K_2(\omega)$ with ωC_r. Of particular interest is the comparison of the radiation damping ratios. At the fundamental system frequency $\bar{\omega}_1$, which was analytically computed to be 2π x 5 Hz and 2π x 5.2 Hz for the EW and NS directions, respectively, the effective EW radiation damping ratios for the frequency-dependent impedance are:

$$D_x(\bar{\omega}_1 = 2\pi \times 5 \text{ Hz}) = 60\%$$
$$D_r(\bar{\omega}_1 = 2\pi \times 5 \text{ Hz}) = 28\%$$

As the frequency exceeds the fundamental mode frequency, the effective radiation damping ratio for the frequency-dependent impedance will also increase, as suggested by Fig. 5-1.

5.1.4 Frequency and Composite Modal Damping

The authors established a mathematical model for the structure, and assumed that the structural modal damping β_j is 2% for all modes. the interaction system was coupled with the frequency-dependent foundation impedances and analyzed by the method of complex modal analysis. This method produced the rigorous solutions for the system frequency and the composite

modal damping. They are compared with the experimental values in the following table, for the first mode only.

	EW		NS	
	$\bar{\omega}_1$	$\bar{\beta}_1$	$\bar{\omega}_1$	$\bar{\beta}_1$
Theory	5.0 Hz	17.7%	5.2 Hz	19.8%
Experiment	4.8 Hz	22.5 to 28.3%* (Ave. = 24.6%)	5.0 Hz	17.5 to 31.5%* (Ave. = 22.0%)

*The experimental values vary from floor to floor.

5.1.5 Summary

Comparison of the analytical and experimental values for system frequency and composite damping for the first mode justifies the adequacy of the impedance theory. Note that the experimental damping consists of the effects of soil material damping and embedment, while the analytical value represents only the radiation damping from the elastic half-space theory.

From the comparisons of D_x and D_r between the frequency-dependent and frequency-independent impedances, it is reasonable to predict that similar analytical results would be obtained when the frequency-independent impedances are used in the calculations.

5.2 CASE II--HAMAOKA NOS. 1 & 2 BWR REACTOR BUILDINGS (Ref. 19)

Forced vibration tests, similar to those performed on Unit 1 in Case I were conducted on Unit 2 after it was built. More data were collected, but the results are essetially the same as those obtained for Case I. Thus, the authors did not attempt another analytical correlation with the test results. The following points are worth mentioning:

- Through-soil structure-structure interaction appeared to be insignificant, when the data are compared between Ref. 17 and 19.
- By using a regression analysis technique, the authors were able to more precisely identify the various modes, whether highly damped or not. Based on this technique, the modal damping values for the different frequency ranges are as follows:
  - 1 to 4 Hz ..... 40 to 50% (essentially ground movements)
  - 4 to 5.7 Hz 20%
  - 5.7 to 9 Hz ..... 3 to 15%

- Because of the similar experimental results in Cases I and II, Case II provides additional verification of the adequacy of the radiation damping theory.

5.3 CASE III--NUCLEAR SAFETY RESEARCH REACTOR BUILDING (Ref. 20)

5.3.1 Structural Data

Base dimension	: 21 m diam (circular)
Total wt. (mg)	: 7585 ton
Wt. mom. inert. abt. base ($I_o g$)	: 1.01×10^6 t-m^2
Height	: 30 m
Embedment	: 10 m

5.3.2 Foundation Data (Layered Soil Site)

Shear wave velocity	: 400 m/sec, ave.
Shear modulus	: 3.27×10^4 t/m^2 ave.
Unit weight	: 2.0 t/m^3 ave.
Poisson's ratio	: 0.45 ave.

5.3.3 Impedances

The following values were obtained based on Table 2-1:

$K_x = 1.777 \times 10^6$ t/m $K_r = 1.84 \times 10^8$ t-m/rad

$D_x = 36\%$ $D_r = 9.2\%$

5.3.4 Experimental Results

Resonance was observed at 5 and 6 Hz in one horizontal direction and at 5 Hz in the other horizontal direction. The associated damping values were found to be about 15% and 18%, respectively.

5.3.5 Summary

The experimental value of the composite modal damping is smaller than that in Case I. The analytical values for D_x and D_r, the impedance damping ratios, are also smaller than those in Case I. Thus, reasonable agreement between the experimental and analytical composite modal damping values can be anticipated although the latter was not available from Ref. 20.

5.4 CASE IV--CONCRETE SLAB FIELD TESTS AT SONGS 2 & 3 SITES (Ref. 21)

To gather realistic soil-structure interaction analysis parameters for the design of Units 2 and 3 of the San Onofre Nuclear Generating Station (SONGS), vibration tests were performed on concrete slabs built at the construction laydown area of the Unit 1 site. Five types of concrete slabs representing different size, embedment condition, and geometry were built (Fig. 5-2). The configuration of the bottom of Slab No. 3 was built to simulate the base slab configuration of a typical PWR containment structure. Additional variations in embedment conditions for Slab Nos. 2 and 3 were considered (Fig. 5-3).

Transient-load vibration tests were conducted. Figure 5-4 shows the mechanism (pull-release) for triggering the slab vibrations. The resultant slab accelerations ranged from 0.2 to 1.0 g, comparable to the anticipated design ground accelerations at the site. The resonant frequency of the slab vibration ranged from 17 to 90 Hz. As expected, the slab motions were typically damped sinusoidal motions.

The near-surface soil is the San Mateo Formation Sand. The shear wave velocity is about 800 to 1200 ft/sec for the top 15 ft of soil, and the averaged value is about 930 ft/sec.

The tests showed essentially the same resonant frequency for both the "horizontal" and rocking modes. Inspection of Figs. 5-2 and 5-4 shows why: for all the horizontal pull tests, the pulling load did not pass through the center of resistance, and significant rocking motion always occurred even though the tests were intended to produce only horizontal-mode slab motions. The slab motion traces shown in Fig. 5-5 for Slab No. 1 clearly confirm this observation.

Appendix A of Ref. 21 describes the details of the slab tests and the resonant frequencies from the various tests. Correlation between the field test results and Table 2-1 impedances is discussed below.

5.4.1 Impedance Springs

When the mass of the slab is known, the effective soil spring constant can be calculated from the observed resonant frequency of the slab. The embedment appeared to have significantly increased the resonant frequency and, hence, the actual soil spring constant.

In general, with shallow or no embedment, the tests suggest that the impedance springs K_x and K_v given in Table 2-1 are sufficient. For the rocking mode, K_r from Table 2-1 appears to overestimate the experimental value. From the analytical point of view, this is also anticipated because, as illustrated in Fig. 5-1, the frequency-dependent impedance spring for the rotational mode is smaller than the K_r from Table 2-1 for the frequency range under consideration. When applied to soil-structure interaction analysis, however, the frequency-independent approximation is still acceptable, as was justified in Ref. 7 for a uniform soil site. Moreover, from the practical point of view, base slabs of the actual structures are all embedded to a certain extent and are seldom purely unembedded. According to the test results, any nominal embedment of the structural base will easily increase the field value of K_r to surpass the analytical value from Tables 2-1 or 2-2.

5.4.2 Impedance Damping

The decay rate of the slab motion provides the value of the equivalent damping ratio, D. Note that the field value includes the combined effects of soil material damping and radiation damping. Comparison of the field and analytical values given by Tables 2-1 or 2-2, which accounts for only the radiation damping, is summarized in Table 5-1.

5.4.2.1 Slab Nos. 1, 2, 4 and 5

For the rotational mode, the analytical radiation damping adequately accounts for the experimental damping. Embedment appears to significantly increase the radiation damping, which is consistent with analytical predictions.

For the horizontal mode, the analytical radiation damping exceeds the experimental value by about 10 to 20%. This is not surprising because, as

mentioned above, the horizontal mode tests produced very strong coupling between the horizontal and rocking motions. Hence, the observed horizontal mode damping was lower than that anticipated on the basis of exciting a pure horizontal mode because the observed damping value represents a certain average of the rocking mode damping and the would-be horizontal mode damping.

For the vertical mode of slab motion, the test results suggest that the effective damping depends strongly on the stress distribution of the soil beneath the slab and on the amplitude of the motion. Note that, in reality, soils do not possess tension capability. During vertical vibrations of substantial amplitude, the bottom of the slab could partially separate from the soil, and the damping would be smaller than that from a low-amplitude vibration. Therefore, it appears reasonable to reduce the analytical radiation damping based on the acceleration of the slab motion.

5.4.2.2 Slab No. 3

This is a peculiar case because the comparison shows the analytical damping value grossly overestimates the field value for all three modes of slab vibration. A correlation between the theory and the field tests appears improbable. Intuitively, one would expect the contrary to occur because the annular ring and block at the bottom of the slab would produce a better "bond" with the soil than would a flat slab bottom.

Because Slab No. 3 was intended to simulate the actual configuration of a typical PWR containment base construction, it is imperative that more test studies be conducted to better understand the effect of the slab bottom configuration on impedance damping.

5.5 CASE V--HARMONIC VIBRATION TESTS ON A STEEL BODY (Ref. 22)

Reference 22 describes harmonic vibration tests conducted on a cubic steel body (1 x 1 x 1 m) that was subjected to different embedment conditions. Figures 5-6 and 5-7 illustrate the test configurations as well as typical footing response vs test frequency curves for the lateral and vertical vibration tests, respectively. Impedance damping for the unembedded case is evaluated here. For the embedded cases, it is apparent that the impedance damping increases with the ratio of embedment of the footing.

5.5.1 LATERAL TEST

In view of the manner in which the lateral vibrarion force was applied, the footing response would be primarily a rocking motion rather than the pure lateral translation o the unembedded case. Therefore, the test value of the damping can be correlated with the analytical rocking mode radiation damping, D_r. The damping value from the test is about 4% of critical for the unembedded case. For the analytical value, the following data are used in the calculation:

Unit wt. of soil	.....	0.13 kip/ft^3
Effective radius, R_r	.....	1.87 ft (based on Table 2-2)
Wt. of footing, W	.....	5.5 kip
Poisson's ratio	.....	0.4
Wt. moment of inertia	.....	$5WR_r^2/3$, approx.

According to Table 2-1, the rocking-mode radiation damping ratio is D_r = 2.8%, which is comparable to the experimental value of 4%.

5.5.2 VERTICAL TEST

The damping from the footing test for the unembedded condition is about 12%. The analytical value, according to Table 2-2, is found to be 35%. Such comparison with the experimental value is similar to that observed in the slab tests in Case IV.

The acceleration of the footing at resonance can be estimated to be about 0.65 g. At such high acceleration, the footing-soil contact condition could substantially differ from that at low acceleration, which would account for the discrepancy between the analytical and the experimental damping values.

TABLE 5-1. Comparison of equivalent damping ratios from analysis and testing.

Slab no.	Data source	Damping ratio D_v	D_x	D_r
1 & 2	A[a]	53%	32%	13%
	F[b]	29 to 60% (8 tests) Ave. = 45%	17 to 44% (13 tests) Ave. = 26%	6 to 20% (14 tests) Ave. = 14%
	$F_{ave.}/A$	0.85	0.81	1.08
3	A	66%	41%	29%
	F	29 to 38% (5 tests) Ave. = 33%	17 to 31% (7 tests) Ave. = 25%	12 to 30% (6 tests) Ave. = 20%
	$F_{ave.}/A$	0.50	0.60	0.69
4 & 5	A	53%	32%	13%
	F	32 to 50%	18 to 40%	10 to 29%
	$F_{ave.}/A$	0.75	0.91	1.46

[a] A = Analytical value based on Table 2-1 or 2-2.
[b] F = Field-test value.

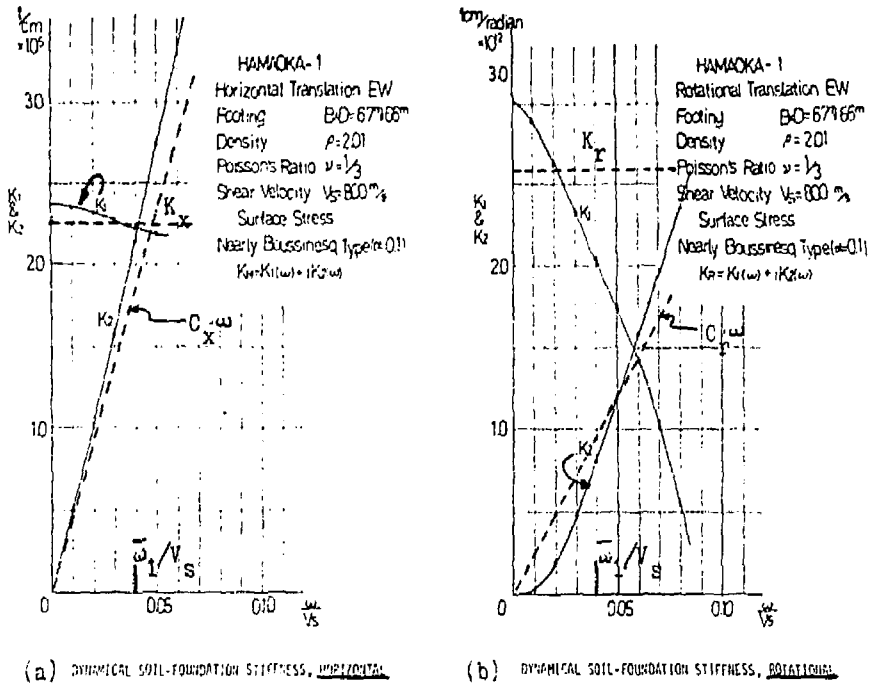

(a) DYNAMICAL SOIL-FOUNDATION STIFFNESS, HORIZONTAL (b) DYNAMICAL SOIL-FOUNDATION STIFFNESS, ROTATIONAL

Fig. 5-i Comparison Between Frequency-Independent Impedances From Table 2-2 And Frequency-Dependent Impedances From Ref. 17 (Case I)

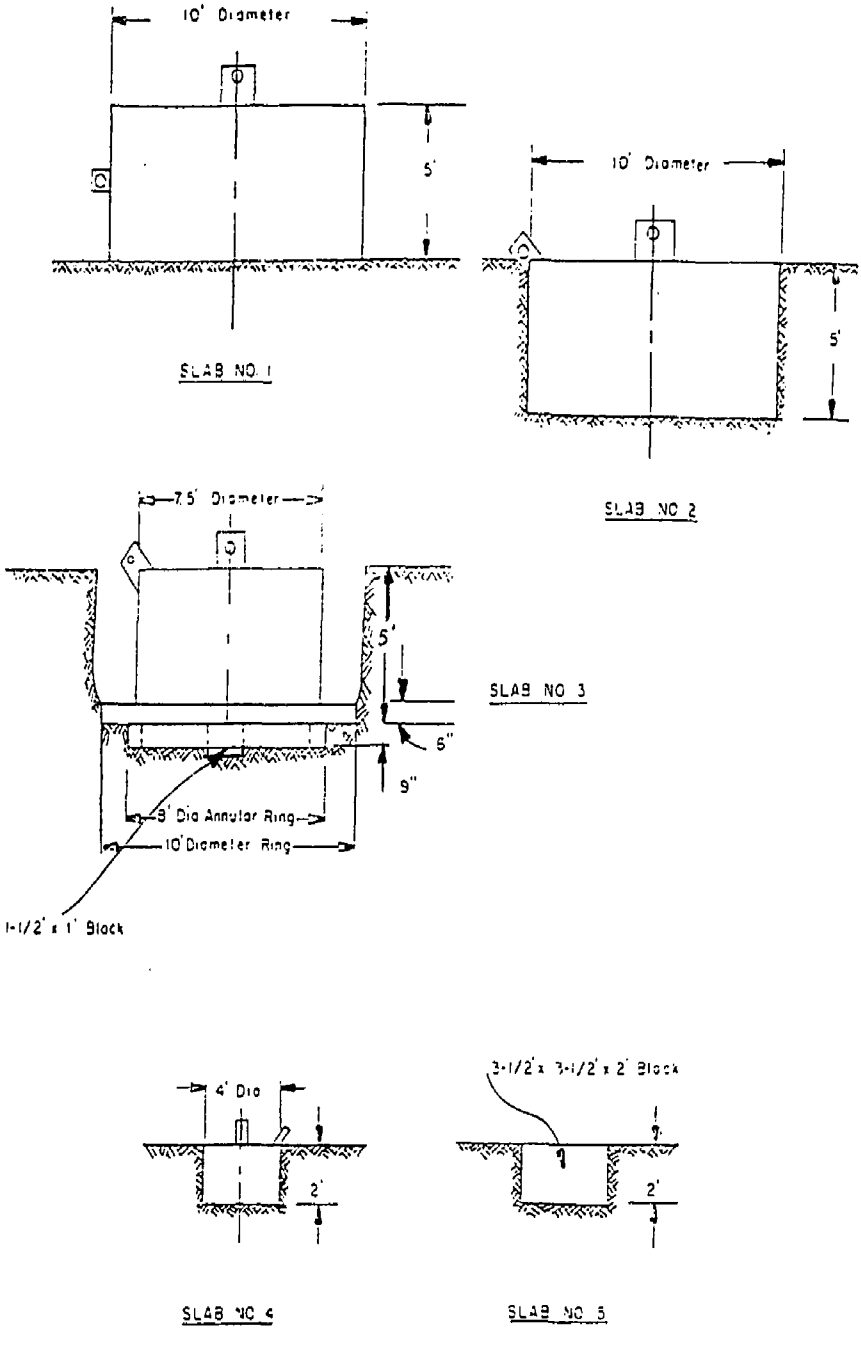

Fig. 5-2 The Five Types of Concrete Slabs in Case IV

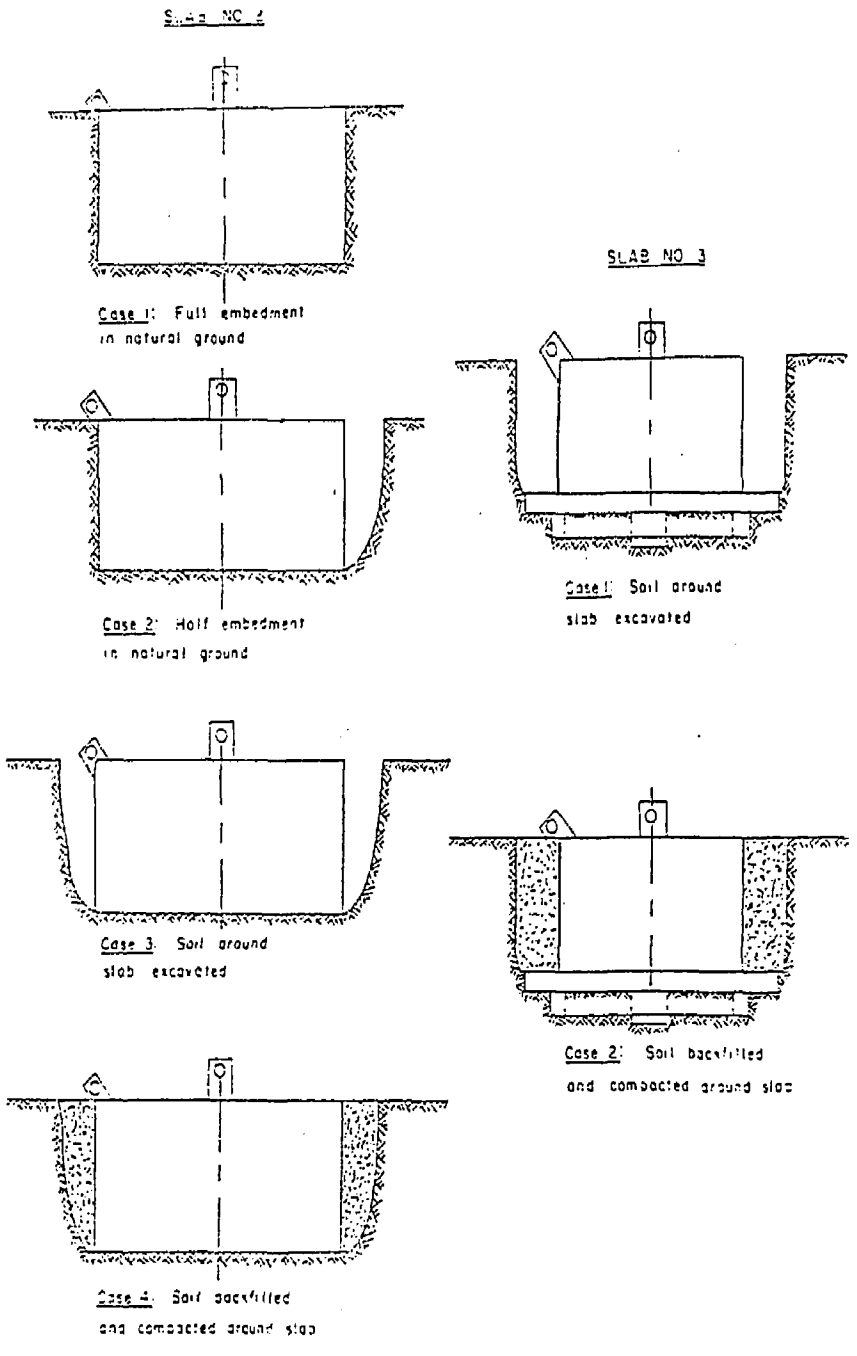

Fig. 5-3 Variation in Embedment Condition for Slab No. 2 and 3 (Reproduced from Ref. 21)

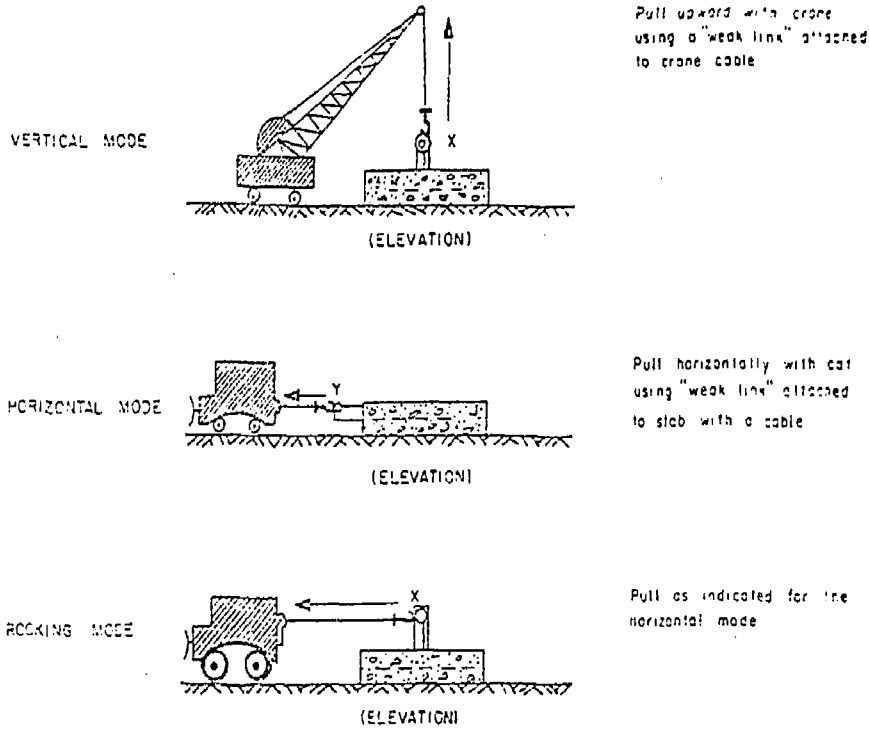

Fig. 5-4 Mechanism for Producing Transient Vibration of the Concrete Slabs (Reproduced from Ref. 21)

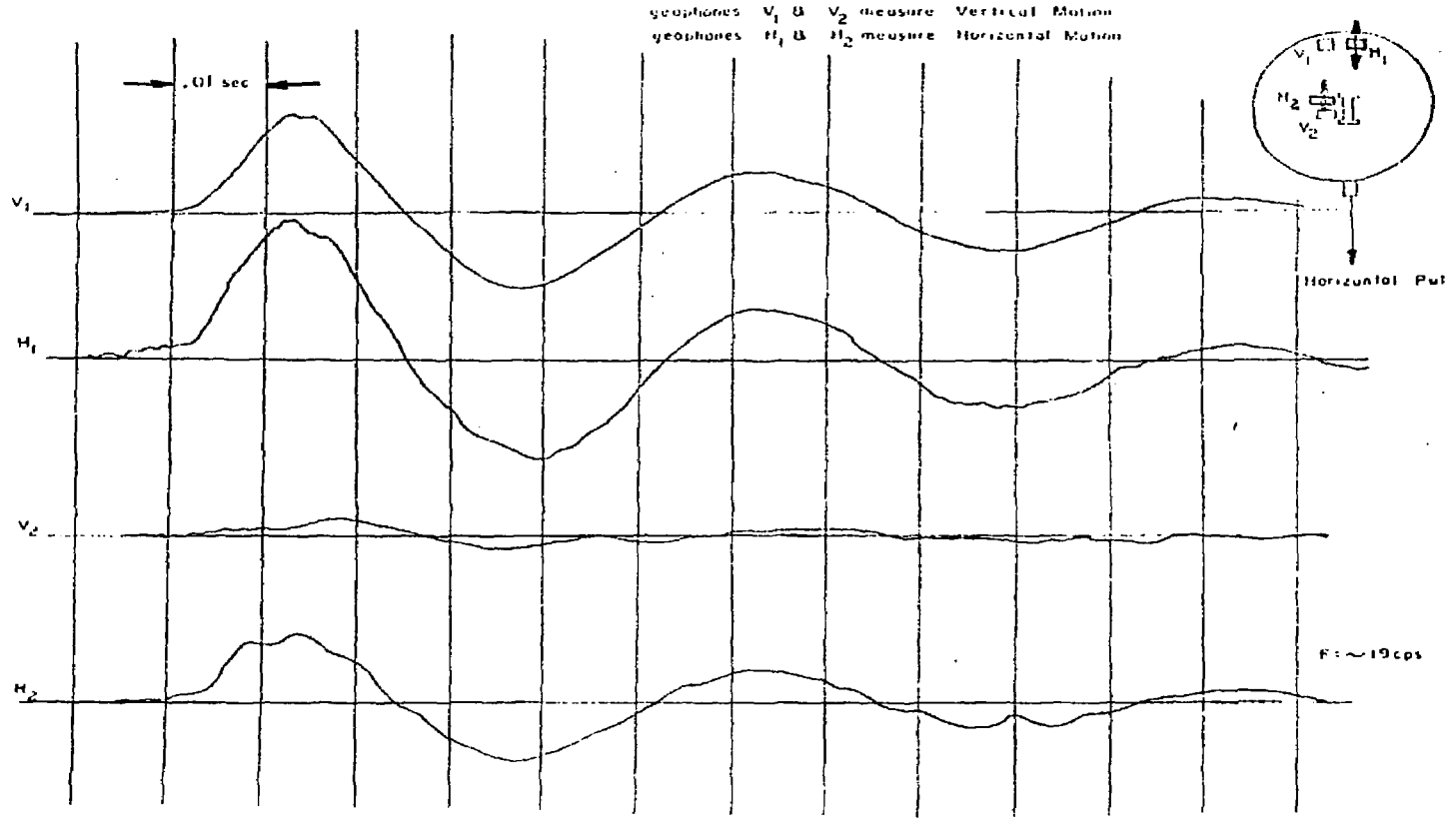

Fig. 5-5 Recorded Slab Velocity Response Traces for Slab No.1 for the Horizontal Mode Pull Test

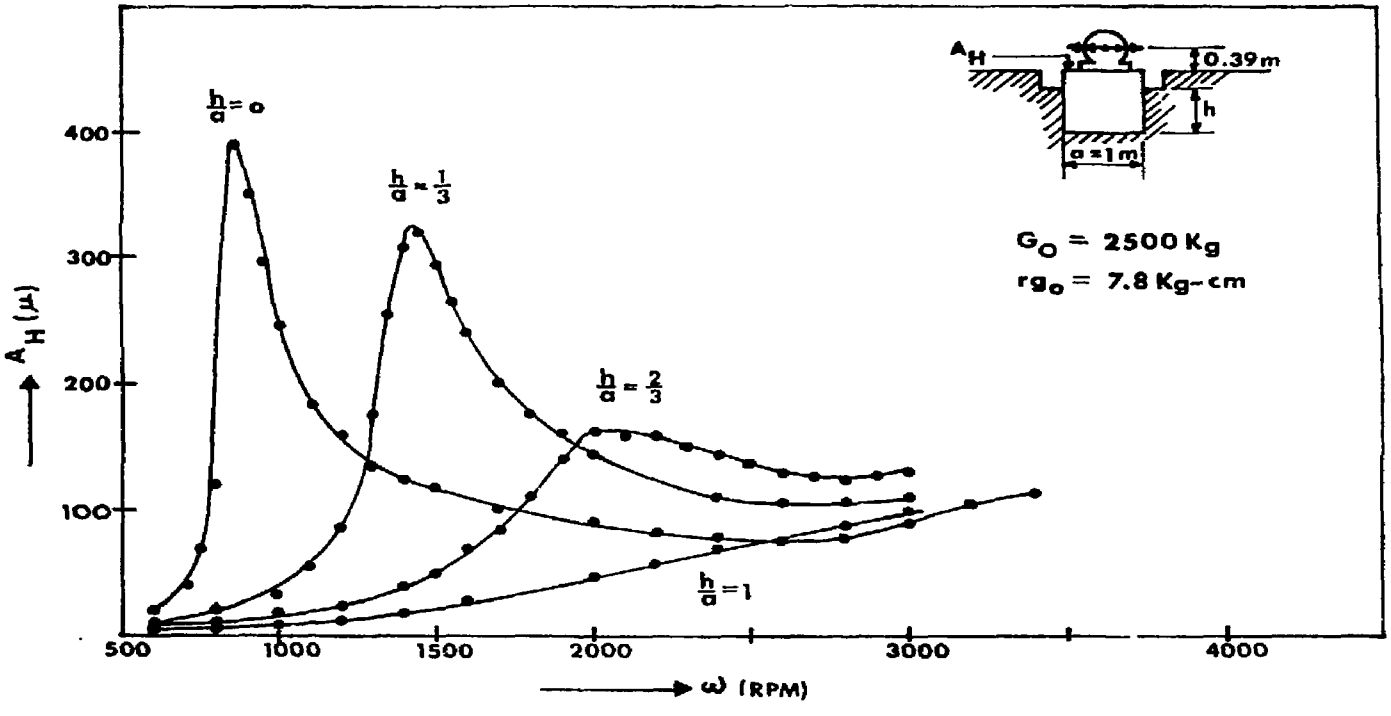

HORIZONTAL VIBRATION RESONANCE CURVES FOR DIFFERENT DEPTHS OF EMBEDMENT, AT SAME MAGNITUDE OF EXISTING FORCES (AFTER NOVAK, 1970)

Fig. 5-6

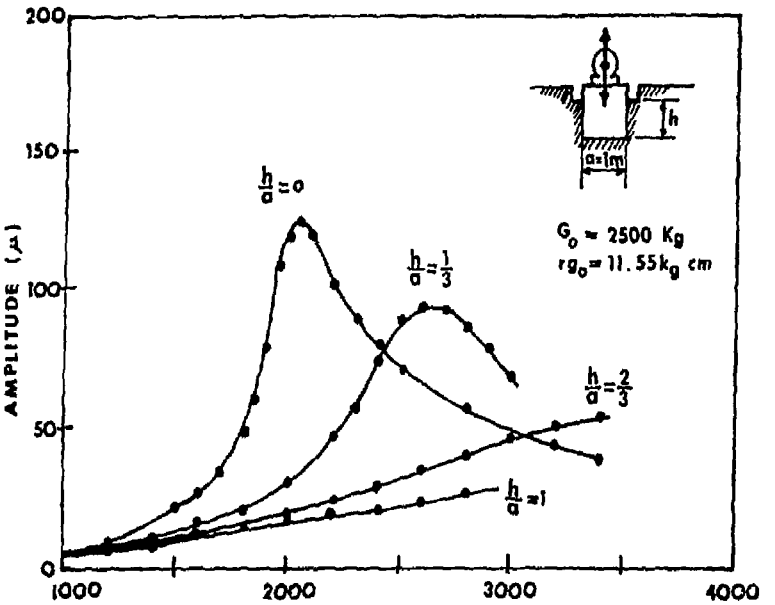

(a) UNDISTURBED SOIL AT SAME MAGNITUDE OF EXCITING FORCES (AFTER NOVAK, 1970)

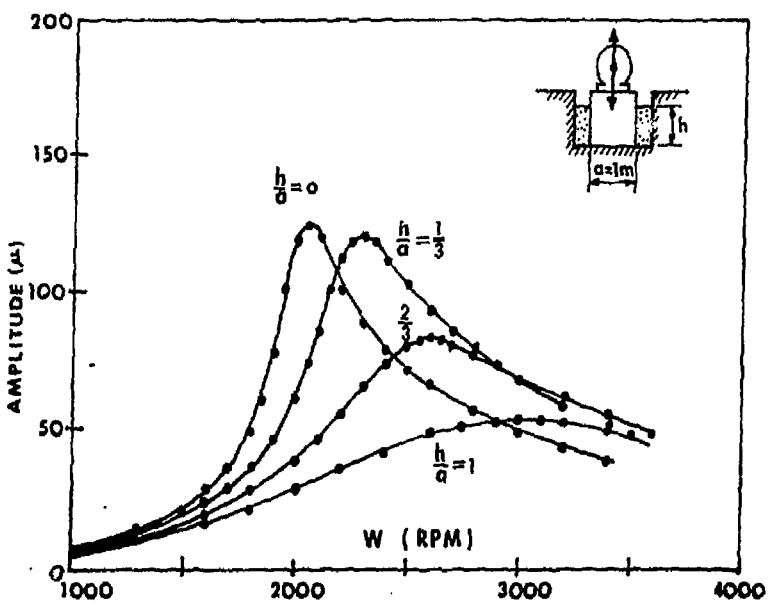

(b) COMPACTED FILL MATERIAL, AT SAME MAGNITUDE OF EXCITING FORCES (AFTER NOVAK, 1970)

Fig. 5-7 Vertical Harmonic Vibration Test of Steel Footing

6. SUMMARY AND CONCLUSIONS

The analytical background and the basic assumptions for the impedance theory were briefly reviewed. The role of radiation damping in soil-structure interaction analysis was discussed. The validity of modeling the soil-structure interaction by using the frequency-independent impedance functions was evaluated based on data from several field-test cases. Finally, the proper procedure for performing soil-structure interaction analyses was discussed with emphasis on the modal superposition method. The limitations of this method were mentioned, and the proper technique for determining composite modal damping was discussed.

The important conclusions and highlights of the discussions are listed below.

6.1 VALIDITY OF THE FREQUENCY-INDEPENDENT IMPEDANCE APPROACH

- For the purpose of analysis, the assumption that the impedance functions are frequency-independent is acceptable for modeling the foundation at sites having fairly uniform soil profiles, but not necessarily for significantly layered sites.

- The impedance springs appear to be adequate representations in accordance with the field tests, and structural embedment effects appear to significantly increase the magnitude of the spring stiffness.

- For the horizontal and rocking modes of a base, the field tests suggest that analytical radiation damping alone is sufficient to represent the combined effects of soil material damping and actual radiation damping in the field. The only exception appears to be Slab No. 3 in Case IV, for which the analytical radiation damping overestimated the observed value. More tests on slabs of similar configuration are recommended.

- According to the field tests, the impedance damping appears to be sensitive to the amplitude of the base vibration for the vertical mode of base vibration, probably because the theory assumes tension capability for the soil in the derivation of impedance. The analytical radiation damping for vertical vibration, therefore, appears to have

overestimated that observed in field tests and should probably be scaled down in proportion to the anticipated structural base acceleration in actual applications. Based on the limited information from Cases IV and V, the scale factor may be on the order of $1 - a_g$, where a_g is the ground acceleration expressed in units of g.

6.2 THE EFFECT OF RADIATION DAMPING ON STRUCTURAL RESPONSE

It was pointed out and demonstrated by examples that the magnitude of the structural response is by no means inversely proportional to the magnitude of the conventionally defined radiation damping ratio, D. Consequently, *arbitrarily reducing the radiation damping does not warrant a more* conservative structural response. Moreover, floor spectra with erroneous peak frequencies could result from such arbitrary reductions.

6.3 ANALYSIS PROCEDURE

The following comments apply to analysis by modal superposition (the normal mode method):

- When frequency-independent impedance functions are used to model the foundation, the normal mode method produces only approximate solutions; the acceptability of such solutions depends largely on the magnitude of the radiation damping. To obtain the rigorous solutions, one can use the methods of Fourier transformation, complex modal analysis, or direct integration.

- When the normal mode method is acceptable, it is important to use the appropriate technique for determining the composite modal damping in order to produce the best approximate solutions. Most existing techniques tend to overestimate the composite modal damping and result in unconservative structural response.

- Given that the normal mode method is acceptable for a problem, and given that an appropriate technique is used to estimate the composite modal damping, the modal damping so determined need not be reduced. Any

drastic reduction in the damping for highly damped modes will only result in extra peaks in the floor spectra--an important point that has been illustrated both analytically and experimentally.

7. REFERENCES

1. Lysmer, J. and Kuhlemeyer, R. L., "Finite Element Model for Infinite Media," Jour. Eng. Mech. Div., ASCE, Vol. 95, No. EM4, Aug. 1969, pp. 859-877.
2. Kausel, E., Roesset, J. M., and Wass, G., "Dynamic Analysis of Footings on Layered Media," Jour. Eng. Mech. Div., ASCE, Vol. 101, No. EM5, Oct. 1975, pp. 679-693.
3. Tseng, W. S. and Tsai, N. C., "Soil-Structure Interaction for Transient Loads Due to Safety Relief Valve Discharge," 4th Int. Conf. Struct. Mech. in Reactor Tech., San Francisco, Calif., Aug. 15-19, 1977.
4. Lysmer, J., Udaka, T., Seed, H. B., and Hwang, R., Complex Response Analysis of Soil-Structure Systems by the Finite Element Method, EERC Report, Univ. of Calif. at Berkeley, 1974.
5. Tsai, N. C., Influence of Local Geology on Earthquake Ground Motions, Ph.D. Thesis Dissertation, Caltech, Pasadena, Calif., June 1969.
6. Schnabel, P. B., Lysmer, J., and Seed, H. B., "Earthquake Response Analysis of Horizontally Layered Sites, EERC Report, Univ. of Calif., Berkeley, 1972.
7. Tsai, N. C., Niefoff, D., Swatta, M., and Hadjian, A. H., "The Use of Frequency-Independent Soil-Structure Interaction Parameters," Nuclear Engineering & Design, Vol. 31, 1974, pp. 168-183.
8. Richart, Jr., F. E., Hall, Jr., J. R., and Woods, R. D., Vibration of Soils and Foundations, Prentice Hall, Inc., 1970, pp. 347 and 382.
9. Luco, J. E., "Vibrations of a Rigid Disc on a Layered Viscoelastic Medium," Nuclear Eng. & Design, Vol. 36, 1976, pp. 325-340.
10. Kausel, E. and Roesset, J. M., "Dynamic Stiffness of Circular Footings," Jour. Eng. Mech. Div., ASCE, Vol. 101, No. EM6, Dec. 1975, pp. 771-785.
11. Novak, M., "Vibrations of Embedded Footings and Structures," Preprint #2029, ASCE Nat. Struct. Eng. Meeting, San Francisco, Calif., April 9-13, 1973.
12. Tsai, N. C., A Discussion of Agrawal's Paper: "Comparative Study for Soil-Structure Interaction Effect by the Soil Spring and Finite Element Model," Technical Paper, Bechtel Power Corporation, San Francisco, Calif., Oct., 1973.
13. Tsai, N. C., "Modal Damping for Soil-Structure Interaction," Jour. Eng. Mech. Div., ASCE, Vol. 100, No. EM2, April 1974, pp. 323-341.

14. Roesset, J. M., Dobry, R., and Whitman, R. V., "Modal Analysis for Structures with Foundation Interaction," Jour. Struct. Div., ASCE, Vol. 99, No. ST3, March 1973.

15. Whitman, R. V., "Soil-Structure Interaction," Seismic Design for Nuclear Power Plants, R. J. Hansen, ed., MIT Press, Cambridge, Mass., 1970, pp. 241-269.

16. Whitman, R. V., Protonotarios, J. N., and Nelson, M. F., "Case Study of Soil-Structure Interaction," Presented at Oct. 16-22, 1972 ASCE Annual & National Environmental Engineering Meeting, Houston, Texas, Preprint #1816.

17. Mizuno, N. and Tsushima, Y., "Experimental and Analytical Studies for a BWR Nuclear Reactor Building Evaluation of Soil-Structure Interaction Behavior," Proc. 3rd SMIRT Conf., London, 1975, Paper K3/2.

18. Tajimi, H., "Interaction of Building and Ground," Earthq. Eng., Nov. 1968, Shokokusha Publishing Co.

19. Mizuno, N., Moribe, I., Suziyama, N., Tsushima, Y., Kushida, H., and Tamabi, T., "Forced Vibration Test of BWR Type Nuclear Reactor Buildings Considering Through Soil Coupling Between Adjacent Buildings," Proc. 5th SMIRT Conf., Berlin, August, 1979, Paper K13/4.

20. Hirasawa, M., Okajima, S., and Satoh, K., "Dynamic Behavior of a Nuclear Reactor Building," Proc. 4th SMIRT Conf., San Francisco, Calif., Aug. 1977.

21. Appendix 3.7C, Soil-Structure Interaction Parameters, Development of Soil-Structure Intraption Parameters for Proposed Units 2 and 3, San Onofre Generation Station for Southern California Edison Co., by Woodward, McNeill & Assoc., Jan. 31, 1971, Final Rev.

22. Novak, M., "Prediction of Footing Vibrations," Jour. Soil Mech. Div., ASCE, Vol. 96, No. SM3, May 1970.